Chemical Science

ROYAL SOCIETY OF CHEMISTRY

EDGE ARTICLE

View Article Online
View Journal | View Issue

Cite this: *Chem. Sci.*, 2020, **11**, 7260

All publication charges for this article have been paid for by the Royal Society of Chemistry

Palladium-catalyzed synthesis of β-hydroxy compounds *via* a strained 6,4-palladacycle from directed C–H activation of anilines and C–O insertion of epoxides†

Raju S. Thombal,[a] Taisiia Feoktistova,[b] Gisela A. González-Montiel,[b] Paul H.-Y. Cheong *[b] and Yong Rok Lee *[a]

Received 11th March 2020
Accepted 20th June 2020

DOI: 10.1039/d0sc01462a

rsc.li/chemical-science

A palladium-catalyzed C–H activation of acetylated anilines (acetanilides, 1,1-dimethyl-3-phenylurea, 1-phenylpyrrolidin-2-one, and 1-(indolin-1-yl)ethan-1-one) with epoxides using *O*-coordinating directing groups was accomplished. This C–H alkylation reaction proceeds *via* formation of a previously unknown 6,4-palladacycle intermediate and provides rapid access to regioselectively functionalized β-hydroxy products. Notably, this catalytic system is applicable for the gram scale mono-functionalization of acetanilide in good yields. The palladium-catalyzed coupling reaction of the *ortho*-C(sp^2) atom of *O*-coordinating directing groups with a C(sp^3) carbon of chiral epoxides offers diverse substrate scope in good to excellent yields. In addition, further transformations of the synthesized compound led to biologically important heterocycles. Density functional theory reveals that the 6,4-palladacycle leveraged in this work is significantly more strained (>10 kcal mol^{-1}) than the literature known 5,4 palladacycles.

Introduction

Transformative transition metal catalyzed coupling reactions concomitant with C–H functionalization and epoxide C–O insertion have recently been reported in the literature.[1–3] The key enabling structural feature in these reactions is the use of strongly coordinating or bi-dentate directing groups. These pioneering reports all hinge on the use of 5,4-metallacycles (Scheme 1).[1–4] Surprisingly, functionalization *via* 6,4-metallacycles is unknown in the literature. We reveal the first examples of successfully accessing and leveraging 6,4-palladacycles.[5] Specifically, we report a palladium-catalyzed regioselective *ortho*-functionalization of anilines with *O*-coordinating directing groups, such as acetanilides, 1-phenylpyrrolidin-2-one, and 1-(indolin-1-yl)ethan-1-one, with epoxides (Scheme 1). We report the density functional theory study of the complete catalytic cycle and also reveal that the 6,4-palladacycle is more strained than the literature-known 5,4 palladacycles. Importantly, the synthesized β-hydroxy compounds are versatile synthons and can be readily converted into biologically important heterocycles such as indoles.[6]

The C–H functionalization of arenes with various coupling partners has become a promising tool for synthetic chemists.[7] Particularly, epoxides are widely used as alkylating reagents and building blocks in the construction of organic molecules *via* C–H bond functionalization.[8] In the past few decades, significant progress has been made on the regioselective ring-opening of epoxides using a variety of nucleophiles on different catalytic platforms.[9] The construction of C–C bonds by the opening of

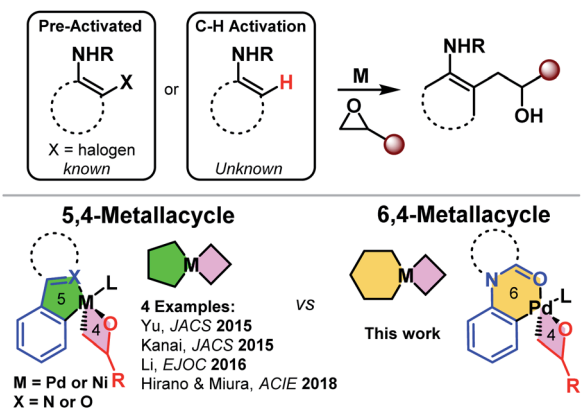

Scheme 1 Transition metal catalyzed C–H/X functionalization and alkylation with epoxides (top) and known 5,4-metallacycle *vs.* the current strategy – 6,4-metallacycle (bottom).

[a]*School of Chemical Engineering, Yeungnam University, Gyeongsan 38541, Republic of Korea. E-mail: yrlee@yu.ac.kr*

[b]*Department of Chemistry, Oregon State University, 153 Gilbert Hall, Corvallis, OR 97331, USA*

† Electronic supplementary information (ESI) available: Experimental procedures, characterization data, computational details and X-ray crystallographic structure and data for **6b-*S***. CCDC 1981280. For ESI and crystallographic data in CIF or other electronic format see DOI: 10.1039/d0sc01462a

epoxides with aryl nucleophiles has played an important role in organic synthesis.[10] Generally, the significant ring strain of epoxides enhances their susceptibility to ring-opening with a wide array of electron-rich species.[11] In this context, several enantioselective and regioselective methods have been developed with the nucleophilic attack of –N, –O, and –halo nucleophiles using the stoichiometric amount of promoters. Therefore, the development of a catalytic version of these types of reactions for the functionalization at a specific position is still highly desirable.

Transition-metal-catalyzed direct utilization of epoxides has received much attention in organic synthesis in the past few decades.[12–15] The reported representative modifications include the nickel-catalyzed opening of epoxides with aryl halides,[16] and Li/Cu-catalyzed synthesis of enantiopure starting materials (Scheme 1).[17]

Results and discussion

To optimize the reaction conditions, we first examined the reaction between *N*-phenylacetamide **1a** and 2-(phenoxymethyl) oxirane **2a** using several catalysts and additives (Table 1). The initial attempts in the presence of 10 mol% of $Ni(COD)_2$, $Rh_2(OAc)_4$, $Co(OAc)_2$, $[RuCl_2(p\text{-cymene})]_2$, and $Cu(OAc)_2$ and 1 equiv. of AcOH in HFIP at 60 °C for 24 h did not provide any products (entries 1–5, Table 1). We also attempted the reaction using several palladium catalysts such as $Pd(TFA)_2$, $PdCl_2$, $Pd(OAc)_2$, and $PdCl_2(PPh_3)_4$ using HFIP as solvent (entries 6–9, Table 1). Among them, the 10 mol% of the $Pd(OAc)_2$ catalyst provided the highest yield (64%). Several solvents were next screened. The reactions using 1,2-dichloroethane, CH_3CN, trifluoroethanol, and tetrahydrofuran as solvents, afforded the desired product **3a** in lower yields, while AcOH failed to produce the desired product (entries 10–14, Table 1). With 1 equiv. of acidic additives PivOH and 1-$AdCO_2H$, **3a** was produced in 31% and 27% yields, respectively (entries 15 and 16, Table 1). With 1 equiv. of basic additives NaOAc or Cs_2CO_3, **3a** was not produced at all (entries 17 and 18, Table 1). Interestingly, increasing the loading of AcOH to 3 equiv. produced the best yield (79%, entry 19, Table 1). However, decreasing the amount of AcOH to 0.5 equiv. provided **3a** in a lower yield (41%, entry 20, Table 1). Overall, acidic additives were found to be superior to basic additives, probably due to their participation in the C–H activation step. Increasing or decreasing the amount of the $Pd(OAc)_2$ catalyst did not improve the yield of **3a** (entries 21 and 22, Table 1). Importantly, the control reaction without the $Pd(OAc)_2$ catalyst failed to produce **3a**. The structure of synthesized compound **3a** was identified by ^1H NMR – there is a characteristic singlet signal of the NH-proton of the acetanilide amide at δ 9.23 ppm and newly generated methine proton

Table 1 Optimization of reaction conditions[a]

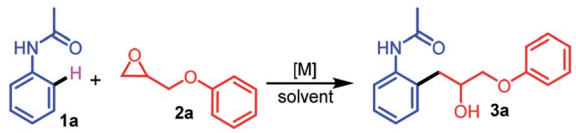

Entry	Catalyst (mol%)	Additives (equiv.)	Solvent	Temp. (°C)	Time (h)	Yield[b] (%)
1	$Ni(COD)_2$ (10)	AcOH (1)	HFIP	60	24	00
2	$Rh_2(OAc)_4$ (10)	AcOH (1)	HFIP	60	24	00
3	$Co(OAc)_2$ (10)	AcOH (1)	HFIP	60	24	00
4	$[RuCl_2(p\text{-cym})]_2$ (10)	AcOH (1)	HFIP	60	24	00
5	$Co(OAc)_2$ (10)	AcOH (1)	HFIP	60	24	00
6	$Pd(TFA)_2$ (10)	AcOH (1)	HFIP	60	24	42
7	$PdCl_2$ (10)	AcOH (1)	HFIP	60	24	38
8	$Pd(OAc)_2$ (10)	AcOH (1)	HFIP	60	24	64
9	$PdCl_2(PPh_3)_4$ (10)	AcOH (1)	HFIP	60	24	54
10	$Pd(OAc)_2$ (10)	AcOH (1)	DCE	80	48	10
11	$Pd(OAc)_2$ (10)	AcOH (1)	CH_3CN	70	48	08
12	$Pd(OAc)_2$ (10)	AcOH (1)	TFE	70	48	10
13	$Pd(OAc)_2$ (10)	—	AcOH	60	48	00
14	$Pd(OAc)_2$ (10)	AcOH (1)	THF	60	48	15
15	$Pd(OAc)_2$ (10)	PivOH (1)	HFIP	60	24	31
16	$Pd(OAc)_2$ (10)	1-$AdCO_2H$ (1)	HFIP	60	24	27
17	$Pd(OAc)_2$ (10)	NaOAc (1)	HFIP	60	24	00
18	$Pd(OAc)_2$ (10)	Cs_2CO_3 (1)	HFIP	60	24	00
19	**$Pd(OAc)_2$ (10)**	**AcOH (3)**	**HFIP**	**60**	**24**	**79**
20	$Pd(OAc)_2$ (10)	AcOH (0.5)	HFIP	60	24	41
21	$Pd(OAc)_2$ (20)	AcOH (3)	HFIP	60	24	79
22	$Pd(OAc)_2$ (05)	AcOH (3)	HFIP	60	24	66
23	—	AcOH (3)	HFIP	60	24	00

[a] Reaction conditions: **1a** (1 mmol), **2a** (1 mmol), catalyst and additives in solvent (3.0 mL) for 24 h. [b] Isolated yields.

at δ 4.25 ppm. The ^{13}C NMR spectrum showed a characteristic signal of the amide carbonyl at δ 168.9 ppm. The structure was further confirmed by single-crystal X-ray diffraction analysis of the structurally related compound **6b-*S***.

In order to explore the mechanism of this reaction, we computed the entire catalytic cycle using DFT – ωB97XD[18]/6-31G* (ref. 19) & LANL2DZ[20]/PCM[21] (acetone)[22] at 60 °C with Gaussian 16. All possible ligand coordination spheres around Pd, involving acetate, acetic acid, acetanilide **1a**, and methyl epoxide for all pathways were considered. This reaction can first proceed *via* $Pd(OAc)_2$ C–H activation of acetanilide **1a** or $Pd(OAc)_2$ C–O insertion into methyl epoxide. All possible routes towards the product were computed,[23] and the proposed catalytic cycle with the resulting minimum energy reaction coordinate is shown in Fig. 1A.[24] The most favored pathway involved first C–H activation of **1a**, followed by C–O insertion of methyl epoxide, and finally reductive elimination to release the product as shown in the reaction coordinate diagram in Fig. 1B.

The catalytic cycle begins with $Pd(OAc)_2$ coordinating to the carbonyl oxygen of the amide **1a** (**Pd-1a-Complex-I**). Subsequent C–H activation ($\Delta G^{\ddagger} = 23.3$ kcal mol^{-1}) leads to the formation of 6-membered **Palladacycle-III** ($\Delta G = -1.5$ kcal mol^{-1}). The C–H activation occurs *via* deprotonation of an ortho-hydrogen of **1a** by a Pd-bound acetate (**CH-Act-TS-II**), rather than direct insertion of Pd into the C–H bond. Epoxide coordination leads to **Palladacycle-Epoxy-Complex-IV** ($\Delta G = -3.1$ kcal mol^{-1}). Oxidative addition into the C–O bond (**CO-Insertion-TS-V**, $\Delta G^{\ddagger} = 31.1$ kcal mol^{-1}) leads to the formation of **6,4-Palladacycle-VI** ($\Delta G = 19.4$ kcal mol^{-1}).[25] Reductive elimination (**Red-Elim-TS-VII**, $\Delta G^{\ddagger} = 30.0$) leads to the **Pd-Prod-Complex-VIII** ($\Delta G = -25.1$ kcal mol^{-1}). The transfer of the palladium catalyst to a new acetanilide substrate is endergonic by 4.2 kcal mol^{-1}.

One of the key features of the title reaction is the expansion into accessing and leveraging 6,4-palladacycles in reactions over the 5,4-palladacycles known in the literature (Scheme 1). We therefore explored the stability of the **6,4-Palladacycle-VI** *vs.* the analogous 5,4-palladacycle derived from 2-phenylpyridine in an isodesmic reaction (Scheme 2).[3] The DFT results reveal that the

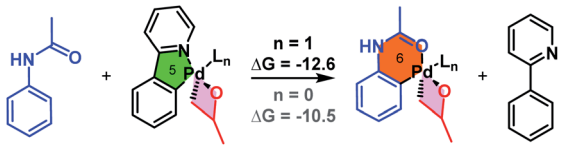

Scheme 2 Isodesmic reaction of 6,4-Palladacycle-VI and the analogous 5,4-palladacycle derived from 2-phenylpyridine.

6,4-palladacycle is higher in energy and more strained than the literature known 5,4 palladacycles by >10 kcal mol^{-1}. This is in line with the slightly elevated temperatures required compared to the Kanai conditions involving the 2-phenylpyridine substrate.[3a]

It is noteworthy that given the significantly greater strain of the 6,4-palladacycle we were able to successfully engage it productively in the current methodology. We hypothesize that the greater strain of this palladacycle contributes to significantly elevating the barrier of the **CO-Insertion-TS-V**, in contrast to other reactions involving the 5,4-palladacycle where C–H activation is considered the rate-determining step (Fig. 2).[3]

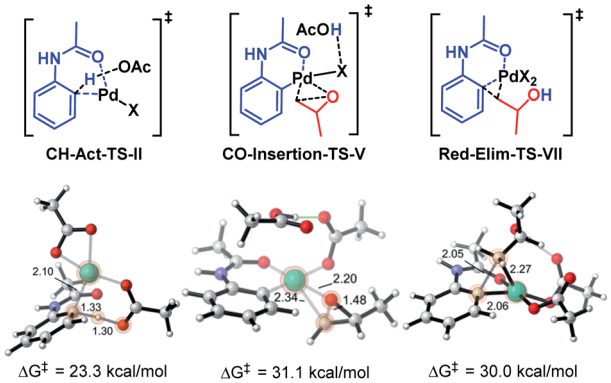

Fig. 2 C–H activation, C–O insertion, and reductive elimination transition structures.

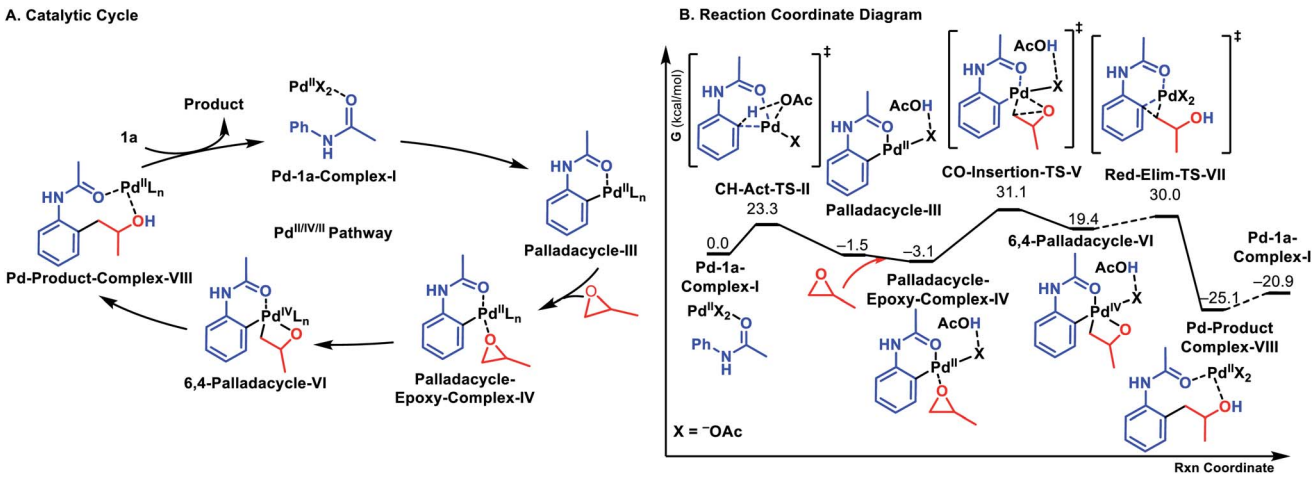

Fig. 1 (A) Proposed catalytic cycle. (B) DFT reaction coordinate diagram for the title reaction. Energies in kcal mol^{-1}.

We extensively investigated the possibility of a Pd(II)-dimer mechanism, as has been reported by Ritter and Sanford among others (for details see the ESI†).[26] Rather, we discovered that the dimer mechanism proceeds *via* a concerted C–O bond breaking and C–C bond forming reductive elimination processes. Despite extensive efforts to locate a stepwise pathway, the dimeric stepwise transition structures were not stationary points on the potential energy surface. The lowest energy concerted Pd dimer reductive elimination barrier was 44.5 kcal mol^{-1}, which was ~15 kcal mol^{-1} higher than the monomer rate-determining step barrier.[27]

To explore the generality of this protocol, further reactions of different epoxides **2b–2k** with **1a** were next examined (Table 2). Treatment of **1a** with several epoxides **2b–2e** bearing electron-donating groups on the benzene ring, such as 4-methoxy, 4-*t*-butyl, 2-methyl, and 2-phenyl under optimized conditions provided the desired products **3b–3e** in excellent yields (76–79%). Similarly, treatment of **1a** with epoxides **2f** or **2g** bearing electron-withdrawing groups 4-Cl and 2,4-Br provided the desired products **3f** and **3g** in 74% and 71% yields, respectively. The reactions of epoxides bearing aliphatic substituents were also tolerated (**3h** and **3i** in 81% and 80% yields, respectively). The reactions of epoxides bearing aliphatic substituents afforded the desired products in higher yields compared to the epoxides bearing aromatic substituents. The reaction of epoxide **2j** bearing a benzyl substituent with **1a** provided the desired alkylated product **3j** in 78% yield. Importantly, the reaction of di-substituted epoxide **2k** with **1a** provided the desired alkylated product **3k** containing a quaternary carbon in good yield (69%).

Table 2 Substrate scope of substituted epoxides **2b–2k**

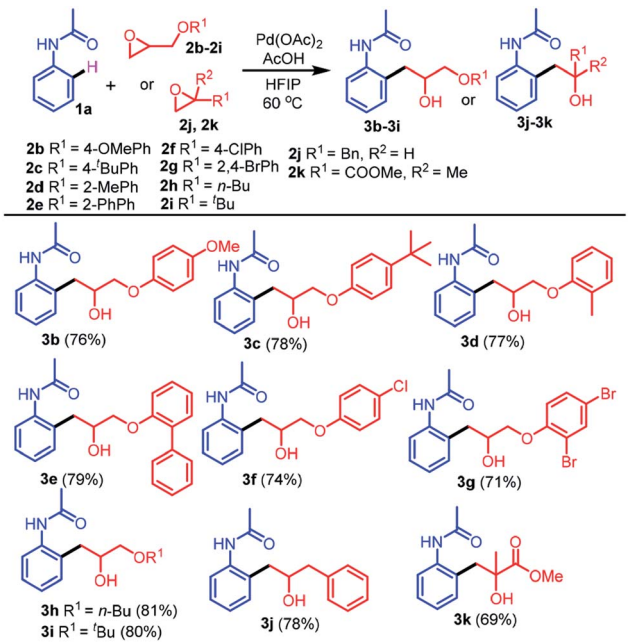

Table 3 Substrate scope of substituted acetanilides **1b–1j**

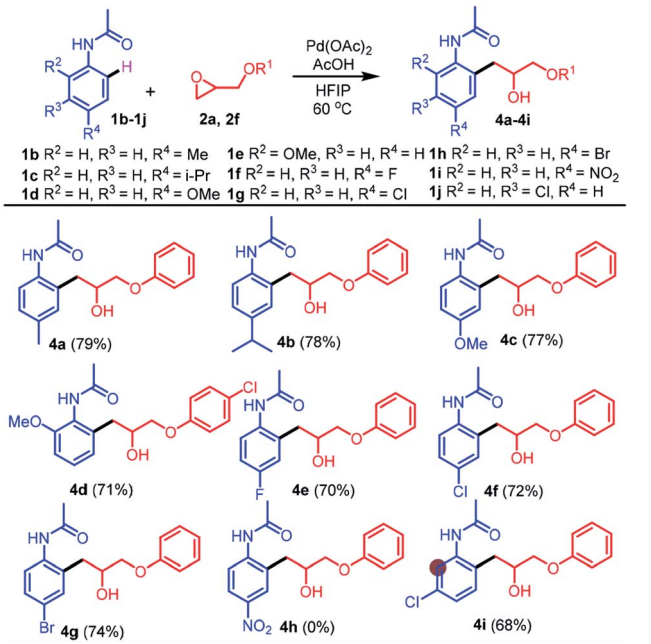

Next, the scope of this reaction was further explored using other substituted acetanilides **1b–1j** bearing various electron-donating and -withdrawing groups on the benzene ring (Table 3). For example, the reaction of **1b–1e** bearing electron-donating groups on the benzene ring at the 2 or 4-position with **2a** or **2f** afforded the expected products **4a–4d** in 71–79% yields. Similarly, the reaction of **1f–1h** bearing *para*-F, -Cl, or -Br groups with epoxide **2a** led to the desired products **4e–4g** in 70–74% yields. However, with **1i** bearing a strong *para* electron-withdrawing nitro group, the desired product **4h** was not isolated, probably due to strong deactivation of the *meta*-position of the nitro group on **1i**. Interestingly, the reaction of **1j** bearing a *meta*-Cl group with **2a** regioselectively afforded the product **4i** in 68% yield.

We then investigated the possibility of using 1,1-dimethyl-3-phenylurea **1k**, 1-phenylpyrrolidin-2-one **1l**, and 1-(indolin-1-yl) ethan-1-one **1m** (Scheme 3). Interestingly, the reaction of the different directing groups **1k–1m** with **2a** or **2c** regioselectively afforded the desired products in 64–80% yields.

To further explore the usefulness and broadness of this reaction, we carried out additional reactions using chiral epoxides as coupling partners (Scheme 4). A combination of (*R*)-2-(phenoxymethyl)oxirane (**2a-*R***) with **1a** afforded the product **6a-*R*** in 75% yield (96% ee), whereas that of (*S*)-2-(phenoxymethyl)oxirane (**2a-*S***) with **1a** resulted in product **6b-*S*** in 76% yield (98% ee). Further, the optical rotation study confirms the retention of the stereochemistry in the obtained products. The observed stereochemistry of the compound **6b-*S*** was confirmed by single-crystal X-ray diffraction analysis.

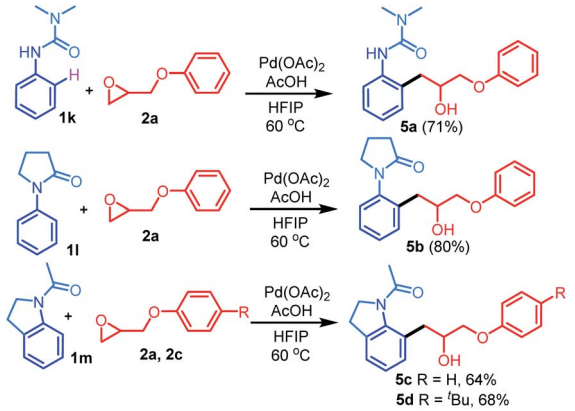

Scheme 3 Reactions of various directing groups **1k–1m** with epoxides **2a** or **2c**.

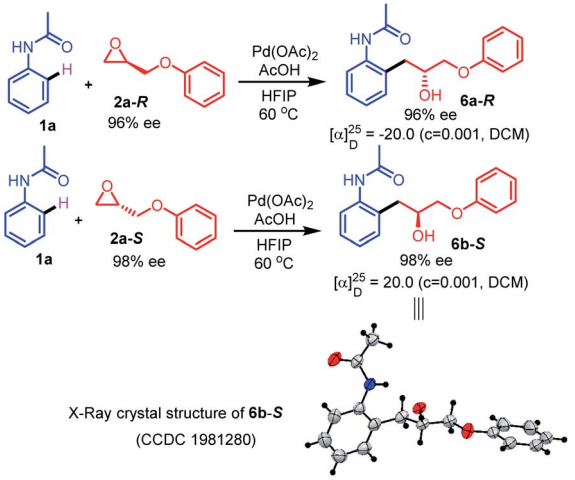

Scheme 4 Reactions of chiral epoxides **2a-*R*** and **2a-*S*** with **1a**.

This new reaction can be carried out on a large scale (for details see the ESI†). To investigate the application of the novel protocol described herein, the conversion of the synthesized compounds **3a** and **3g** into new molecules was attempted (Scheme 5). Surprisingly, pyridinium chlorochromate (PCC) oxidation of **3a** and **3g** led to the direct formation of indoles **7** and **8** in 86 and 92% yields, respectively.

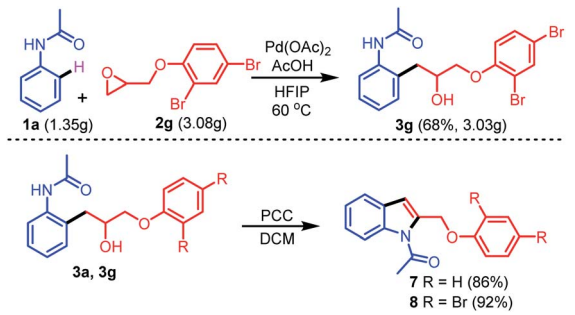

Scheme 5 Gram scale experiment and further transformations of the synthesized compounds **3a**, and **3g** to indoles.

Conclusions

In summary, we have developed palladium-catalyzed regioselective C–H functionalization of *O*-coordinating directing groups with epoxides *via* Pd(II)/(IV)/(II) pathways. This reaction efficiently tolerates chiral epoxides, providing step-economical access to chiral alcohols on the benzene ring with high levels of regio- and stereo-selective control. Other directing groups such as 1,1-dimethyl-3-phenylurea, 1-phenylpyrrolidin-2-one, and 1-(indolin-1-yl)ethan-1-one were also successfully utilized in this transformation. This protocol also provides easy access to biologically important heterocycles with the further transformation of the synthesized compounds. The density functional theory study reveals that the new 6,4-palladacycles engaged in this work are significantly more strained than the literature known 5,4-palladacycles and their successful engagement in productive synthetic processes.

Conflicts of interest

There are no conflicts to declare.

Acknowledgements

This work was supported by the National Research Foundation of Korea (NRF) grant funded by the Korea government (MSIT) (2018R1A2B2004432). This research was supported by the Nano Material Technology Development Program of the Korean National Research Foundation (NRF) funded by the Korean Ministry of Education, Science, and Technology (2012M3A7B4049675). PHYC is the Bert and Emelyn Christensen professor, and gratefully acknowledges financial support from the Vicki & Patrick F. Stone family and the National Science Foundation (NSF, CHE-1352663).

Notes and references

1 S.-B. Xu, K. Takamatsu, K. Hirano and M. Miura, *Angew. Chem., Int. Ed.*, 2018, **57**, 11797–11801.
2 G. Cheng, T.-J. Li and J.-Q. Yu, *J. Am. Chem. Soc.*, 2015, **137**, 10950–10953.
3 (*a*) Z. Wang, Y. Kuninobu and M. Kanai, *J. Am. Chem. Soc.*, 2015, **137**, 6140–6143; (*b*) D.-D. Li, L.-F. Niu, Z.-Y. Ju, Z. Xu and C. Wu, *Eur. J. Org. Chem.*, 2016, **18**, 3090–3096.
4 B. Lian, L. Zhang, S.-J. Li, L.-L. Zhang and D.-C. Fang, *J. Org. Chem.*, 2018, **83**, 3142–3148.
5 Recently, the acetanilides have been widely utilized in the C–H activation reactions. (*a*) X. Wan, Z. Ma, B. Li, K. Zhang, S. Cao, S. Zhang and Z. Shi, *J. Am. Chem. Soc.*, 2006, **128**, 7416–7417; (*b*) C. S. Yeung, X. Zhao, N. Borduas and V. M. Dong, *Chem. Sci.*, 2010, **1**, 331–336; (*c*) R. Giri, J. K. Lam and J.-Q. Yu, *J. Am. Chem. Soc.*, 2010, **132**, 686–693; (*d*) L. Ackermann, L. Wang, R. Wolfram and A. V. Lygin, *Org. Lett.*, 2012, **14**, 728–731; (*e*) G. E. M. Crisenza, O. O. Sokolova and J. F. Bower, *Angew. Chem., Int. Ed.*, 2015, **54**, 14866–14870; (*f*) S. Grélaud, P. Cooper, L. J. Feron and J. F. Bower, *J. Am. Chem. Soc.*,

2018, **140**, 9351–9356; (*g*) R. S. Thombal and Y. R. Lee, *Org. Lett.*, 2020, **22**, 3397–3401.

6 R. D. Taylor, M. MacCoss and A. D. G. Lawson, *J. Med. Chem.*, 2014, **57**, 5845–5859.

7 (*a*) A. Dey, S. K. Sinha, T. K. Achar and D. Maiti, *Angew. Chem., Int. Ed.*, 2019, **58**, 10820–10843; (*b*) S. Rej and N. Chatani, *Angew. Chem., Int. Ed.*, 2019, **58**, 8304–8329; (*c*) D. J. Abrams, P. A. Provencher and E. J. Sorensen, *Chem. Soc. Rev.*, 2018, **47**, 8925–8967; (*d*) N. Thrimurtulu, A. Dey, A. Singh, K. Pal, D. Maiti and C. M. R. Volla, *Adv. Synth. Catal.*, 2019, **361**, 1441–1446; (*e*) H. Kim, R. S. Thombal, H. D. Khanal and Y. R. Lee, *Chem. Commun.*, 2019, **55**, 13402–13405; (*f*) O. Baudoin, *Angew. Chem., Int. Ed.*, 2020, DOI: 10.1002/anie.202001224.

8 (*a*) C.-Y. Huang and A. G. Doyle, *Chem. Rev.*, 2014, **114**, 8153–8198; (*b*) R. E. Parker and N. S. Isaacs, *Chem. Rev.*, 1959, **59**, 737–799; (*c*) I. Vilotijevic and T. F. Jamison, *Angew. Chem., Int. Ed.*, 2009, **48**, 5250–5281; (*d*) C. J. Morten, J. A. Byers, A. R. Van Dyke, I. Vilotijevic and T. F. Jamison, *Chem. Soc. Rev.*, 2009, **38**, 3175–3192; (*e*) E. N. Jacobsen, *Acc. Chem. Res.*, 2000, **33**, 421–431.

9 C. Wang, L. Luo and H. Yamamoto, *Acc. Chem. Res.*, 2016, **49**, 193–204.

10 M. Alam, C. Wise, C. A. Baxter, E. Cleator and A. Walkinshaw, *Org. Process Res. Dev.*, 2012, **16**, 435–441.

11 R. M. Hanson, *Chem. Rev.*, 1991, **91**, 437–478.

12 Y. D. Y. L. Getzler, V. Mahadevan, E. B. Lobkovsky and G. W. Coates, *J. Am. Chem. Soc.*, 2002, **124**, 1174–1175.

13 C. Molinaro and T. F. Jamison, *Angew. Chem., Int. Ed.*, 2005, **44**, 129–132.

14 (*a*) S. Teng, M. E. Tessensohn, R. D. Webster and J. S. Zhou, *ACS Catal.*, 2018, **8**, 7439–7444; (*b*) Y. Ikeda, H. Yorimitsu, H. Shinokubo and K. Oshima, *Adv. Synth. Catal.*, 2004, **346**, 1631–1634.

15 K. M. Miller, T. Luanphaisarnnont, C. Molinaro and T. F. Jamison, *J. Am. Chem. Soc.*, 2004, **126**, 4130–4131.

16 Y. Zhao and D. J. Weix, *J. Am. Chem. Soc.*, 2014, **136**, 48–51.

17 P. T. Marcyk, L. R. Jefferies, D. I. AbuSalim, M. Pink, M. Baik and S. P. Cook, *Angew. Chem., Int. Ed.*, 2019, **58**, 1727–1731.

18 J. Chai and M. Head-Gordon, *J. Chem. Phys.*, 2008, **10**, 6615–6620.

19 W. J. Hehre, R. Ditchfield and J. A. Pople, *J. Chem. Phys.*, 1972, **56**, 2257.

20 (*a*) P. J. Hay and W. R. Wadt, *J. Chem. Phys.*, 1985, **82**, 270–283; (*b*) W. R. Wadt and P. J. Hay, *J. Chem. Phys.*, 1985, **82**, 284–298; (*c*) P. J. Hay and W. R. Wadt, *J. Chem. Phys.*, 1985, **82**, 299–310.

21 (*a*) S. Miertuš, E. Scrocco and J. Tomasi, *Chem. Phys.*, 1981, **55**, 117–129; (*b*) S. Miertuš and J. Tomasi, *Chem. Phys.*, 1982, **65**, 239–245; (*c*) J. L. Pascual-Ahuir, E. Silla and I. Tuñón, *J. Comput. Chem.*, 1994, **15**, 1127–1138.

22 HFIP solvent effects have been successfully modeled using PCM(acetone) and PCM(TFE): (*a*) A. Berkessel, J. A. Adrio, D. Hüttenhain and J. M. Neudörfl, *J. Am. Chem. Soc.*, 2006, **128**, 8421–8426; (*b*) E. Erbing, A. Sanz-Marco, A. Vázquez-Romero, J. Malmberg, M. J. Johansson, E. Gómez-Bengoa and B. Martín-Matute, *ACS Catal.*, 2018, **8**, 920–925.

23 See the ESI† for other pathways considered.

24 Structures involving the acetanilide amide-tautomer were also explored; in B3LYP, the C–H activation transition states of the tautomer were higher in energy by >13 kcal mol^{-1} than the non-tautomer. We were unable to locate a first order saddle point for the C–H activation transition state using wB97XD, but the intermediates prior to the C–H activation are also consistent with the tautomeric form being higher in energy (>9 kcal mol^{-1}). See the ESI.†

25 We also examined the addition of an aryl-Pd nucleophile to the unopened epoxide, which would directly lead to the product catalyst complex without going through the C–O insertion of the epoxide and reductive elimination. The computed barrier for this process is 41.1 kcal mol^{-1}, which is 10 kcal mol^{-1} higher in energy than that of the stepwise process shown in Fig. 1.

26 (*a*) M. A. Gutierrez, G. R. Newkome and J. Selbin, *J. Organomet. Chem.*, 1980, **202**, 341–350; (*b*) N. R. Deprez and M. S. Sanford, *J. Am. Chem. Soc.*, 2009, **131**, 11234–11241; (*c*) D. C. Powers, M. A. Geibel, J. E. Klein and T. Ritter, *J. Am. Chem. Soc.*, 2009, **131**, 17050–17051; (*d*) D. C. Powers and T. Ritter, *Nat. Chem.*, 2009, **1**, 302; (*e*) N. R. Deprez and M. S. Sanford, *J. Am. Chem. Soc.*, 2009, **131**, 11234–11241.

27 Various Pd dimer arrangements as well as *syn*- and *anti*-arrangements of the amides and HFIP as well as acetic acid coordination to the forming alkoxide in the concerted reductive elimination transition structures were computed. Alternate arrangements of the dimer species that are not analogous to the literature precedents were also considered, and they were even higher in energy.